A SUB-DOMAIN TECHNIQUE FOR THE SCATTERING THROUGH SMALL APERTURES

V. GOBIN
ONERA (Office National d'Études et de Recherches Aérospatiales)
2 avenue Belin, BP 4025, 31055 Toulouse cedex 4, France
vincent.gobin@onecert.fr

B. PECQUEUX
CEG (Centre d'Etude de Gramat)
46500 Gramat

Abstract : The objective of this paper is to demonstrate the interest of the introduction of the small aperture hypothesis in the sub-domain technique FACTOPO. First of all, we recall a few results on the dipole approximation for small apertures. Then we introduce the basis of our sub-domain technique FACTOPO and introduce relevant basis functions deduced from the previous hypothesis. A numerical application is proposed to validate the concepts.

1. THEORY

1.1. Recall of some properties for small apertures

We know for a long time and Bethe theory [1], [2], [3] that scattering of an electromagnetic field through a small aperture in an infinite wall can be approximated with two "equivalent dipoles" radiating in free space. Under some hypothesis (aperture size small with respect to wave length, evaluation of the field "far" from the aperture, locally smooth variation of the incident field) we know that the two dipoles are related to the so called "short-circuit fields" via the electric and magnetic polarisabilities : $\begin{cases} \vec{P}_m = -\overline{\alpha}_m \vec{H}_{sc} \\ \vec{P}_e = \varepsilon \overline{\alpha}_e \vec{E}_{sc} \end{cases}$

and are directly calculated as first order moments of the actual distribution of the electric field in the aperture : $\begin{cases} \vec{P}_m = \dfrac{1}{j\omega\mu} \displaystyle\int_S \left(\vec{E}(r') \times \vec{n}\right) dr' \\ \vec{P}_e = -\dfrac{\varepsilon}{2} \displaystyle\int_S \vec{r}' \times \left(\vec{E}(r') \times \vec{n}\right) dr' \end{cases}$

1.2. General description of the sub-domain approach

Now, we describe the sub-domain technique. A three step approach is conducted:

- The first step consists in a breakdown of the initial problem into elementary sub-domains, and the analysis of penetration paths. Then, interfaces between sub-domains are defined. Now, to built a graph associated with the topology of the structure, we represent each sub-domain and each load at the wires by a node, and interfaces by a branch.

- The second step is the characterization of electromagnetic interactions, for each sub-domain, at interface level. Then, a linear relation applied on EM fields can be defined and written as a [Y] matrix. To determine the [Y] matrix of each sub-domain, the $\vec{E}$ field is expanded on interface N_j, of normal vector $\vec{n}^j$, in the following way :

$$\vec{n}^j \times \vec{E} = \sum_{n=1}^{NT(j)} V_n^j \vec{n}^j \times \vec{f}_n^{\,j}$$

where $\vec{f}_n^{\,j}$ are bases functions, $NT(j)$ is the total number of basis functions on interface j, V_n^j are expansion coefficients. Then, the magnetic field can be obtained (with any technique for the solving of Maxwell equation) :

$$\vec{n}\times\vec{H} = \sum_{j=1}^{N_j}\sum_{n=1}^{NT(j)} V_n \vec{n}\times\vec{H}_n^{\,j\,excit} + \vec{n}\times\vec{H}^{\,source}$$

where $\vec{n}\times\vec{H}_n^{\,j\,excit}$ is the obtained response when an electric field equal to base function $\vec{f}_n^{\,j}$ is applied and $\vec{n}\times\vec{H}^{\,source}$ is the response when the actual source of the EM fields is applied. Both $\vec{n}\times\vec{H}_n^{\,j\,excit}$ and $\vec{n}\times\vec{H}^{\,source}$ are evaluated with all the interfaces short-circuited.

And now, if we introduce the product $\langle\vec{a},\vec{b}\rangle = \int \vec{a}.\vec{b}^{\,*}dS$ and test functions $\vec{t}_m^{\,i}$ which are equal to base functions $\vec{f}_n^{\,j}$ (Galerkin's method), we can characterize the sub-domain by means of a [Y] matrix : $[I^p] = [Y][V] + [I^{source}]$

where :
$$\begin{cases} I^{p}{}_m^{\,i} = \langle \vec{n}_j \times \vec{H}, \vec{t}_m^{\,i} \rangle \\ Y_{nm}^{ij} = \langle \vec{n}\times\vec{H}_n^{\,j\,excit}, \vec{t}_m^{\,i} \rangle \\ I^{source}{}_m^{\,i} = \langle \vec{n}_j \times \vec{H}^{\,source}, \vec{t}_m^{\,i} \rangle \end{cases}$$

- The last step is the calculation of the global response. Indeed, thank to the associated graph and applying continuity conditions, a linear system can be built, taking interactions between sub-domains into account. Solving this system leads to the global response for a given excitation.

1.3. Choice of the basis functions

In this paper, we apply successively two kinds of basis functions :

1) Local basis functions directly equal to the Rao-Whitney-Glisson functions [2], as used in most integral equation formalism.
2) Global basis functions deduced from the above small aperture approximations

In this second case, knowing the representation of the scattered fields by means of two magnetic and electric dipoles, we can introduce a parameterization of the E field in the aperture with three contributions : $\vec{n}\times\vec{E} = \sum_{i=1}^{3} V_i \vec{n}\times\vec{E}_i = V_1\vec{n}\times\vec{E}_1 + V_2\vec{n}\times\vec{E}_2 + V_3\vec{n}\times\vec{E}_3$

- where $\vec{M}_1 = \vec{n}\times\vec{E}_1$ (respectively $\vec{M}_2 = \vec{n}\times\vec{E}_2$) is a distribution of magnetic currents that produce the same field as an equivalent unitary magnetic current $\vec{M}_{eq1} = 1$ (respectively $\vec{M}_{eq2} = 1$) in the $\vec{t}_1$ (resp. $\vec{t}_2 = \vec{n}\times\vec{t}_1$) direction;

- where $\vec{M}_3$ is a distribution of magnetic currents that produce the same field as an equivalent unitary magnetic current $\vec{J}_{eq1} = j$ in the normal direction $\vec{n}$

In practice, the distributions are evaluated, solving a secondary problem : the scattering of an incident field through a small aperture in an infinite perfectly conducting wall. We solve Maxwell equations (with an integral equation formalism) for three incidences exciting the wanted field:

- $\vec{M}_1 = \vec{n}\times\vec{E}_1$ and $\vec{M}_2 = \vec{n}\times\vec{E}_2$ are obtained for two incidences that give only a magnetic short-circuit field in the $\vec{t}_1$ and $\vec{t}_2$ directions

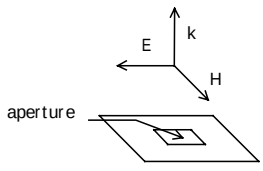

Fig. 1a Incidence for computing $\vec{M}_1 = \vec{n}\times\vec{E}_1$

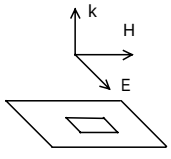

Fig.1b Incidence for computing $\vec{M}_2 = \vec{n}\times\vec{E}_2$

- $\vec{M}_3 = \vec{n} \times \vec{E}_3$ is obtained by calculating the mean value of the fields obtained for two incidences with the same electric short-circuit field and opposite magnetic field, as seen on Fig. 1c.

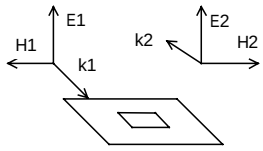

Fig. 1c Incidence for computing $\vec{M}_3 = \vec{n} \times \vec{E}_3$

2. APPLICATION

The validation of the general concept is carried out on a cavity with a 2cm*2cm aperture on the upper side. An internal wire is loaded at both ends with R1 and R2 impedances (50 Ω in the numeric test). An external plane wave is taken as the electromagnetic source. The incidences of interest in the following computations are chosen in order to produce either a pure magnetic short-circuit field (incidence n°1), or a superposition of a E and H fields (incidence n°2) :

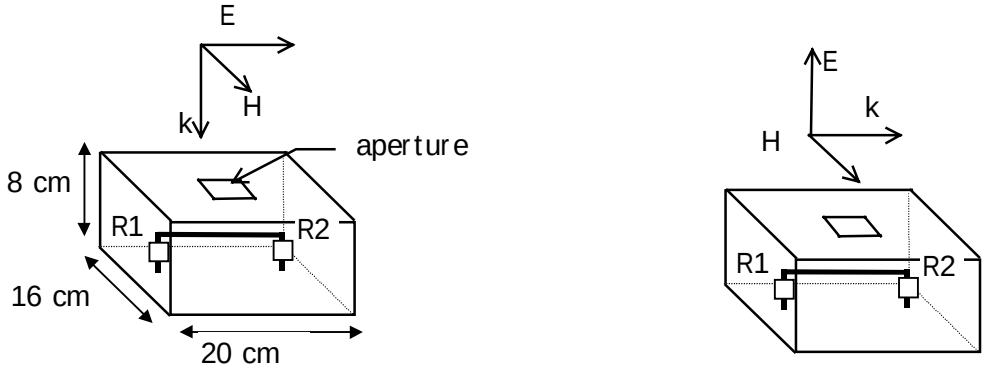

Fig. 2 studied structure for incidence n°1 and 2°

All the following results are obtained with a solver for Maxwell equations based on an integral equation formalism.

2.1. Sub-domain decomposition with local basis functions

The first result is computed with a set of 133 basis functions (one per edge of the mesh) on the aperture. On Fig.3, the associated graph of the structure is plotted. The outside sub-domain, where the source is located, is represented by node 4 and the inner sub-domain, where the reception line is placed, by node 2. Loads at the wires correspond to nodes 1, 3. The framed numbers correspond to matrix size associated to nodes, and numbers in square brackets correspond to number of basis functions by interfaces. Note that the data storage is quite important : $200*16*135^2$=58 Mbytes for keeping the complex [Y] matrix of node 2 for the 200 frequencies of the computation.

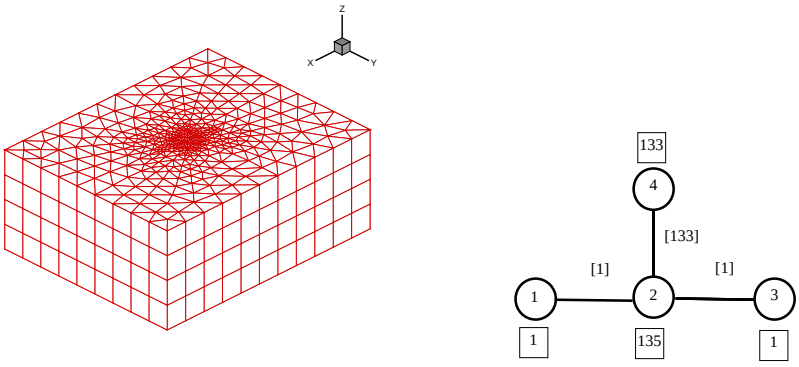

Fig. 3 : mesh of the structure and associated graph

The results are plotted on next figures for the two incidences (with result from a direct calculation for comparison) and we observe a very good agreement.

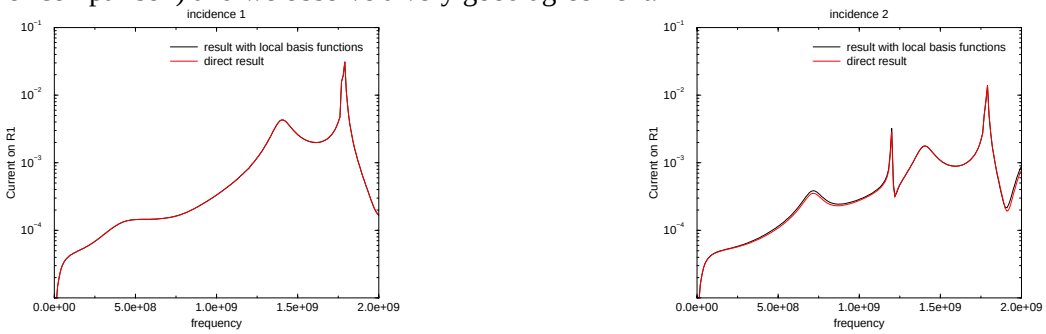

Fig. 4 : results with the local basis-functions

2.2. Sub-domain decomposition with global basis functions

Applying the principle of §1.3, we have obtained the three following basis functions

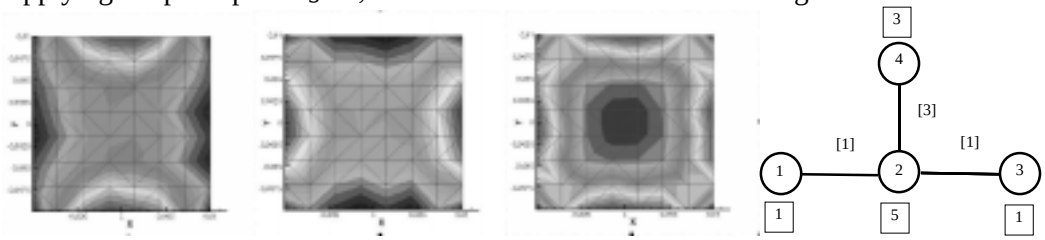

Fig. 5 : representation of the three global functions and the associated graph

The associated graph is quite similar in shape to that of Fig. 3 but the number of basis functions on the aperture is dramatically reduced (133 down to 3). The final results are quite promising (fig. 6) in spite of a 20% discrepancy which origin is still under study.

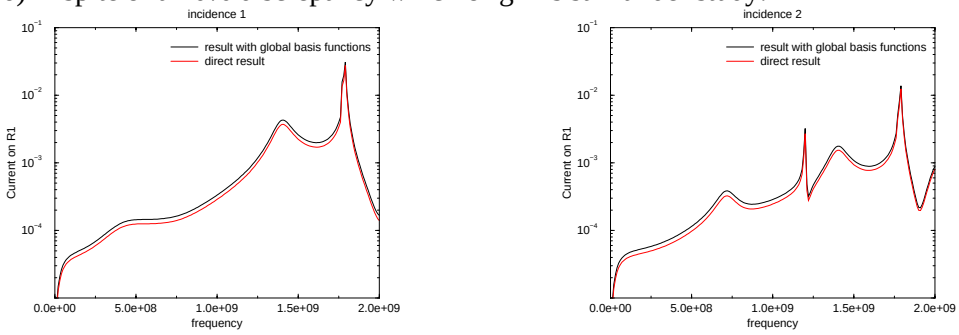

Fig. 6 : results with the local basis-functions

Références :

[1] M. A. Bethe, « Theory of Diffraction by small Holes », Physical Review, Second Series, 66, 7 and 8, pp.163-182, Oct 1. and 15, 1944.

[2] V. Gobin « Diffraction par des ouvertures et des objets tridimensionnels; Application à la mesure des impédances de surface des matériaux bons conducteurs », Thèse d'Electronique de l'Université de Lille Flandres Artois, 3 juillet 1989 (in french).

[3] R. F. Harrington « Resonant Behavior of a Small Aperture backed by a Conducting Body ». IEEE Transactions on Antennas and Propagation, vol AP-30,n°2, March 1982.